Original Article

JCBFM

Journal of Cerebral Blood Flow & Metabolism
2021, Vol. 41(12) 3288–3301

DOI: 10.1177/0271678X211029060
journals.sagepub.com/home/jcbfm
SAGE

Nrf2-BDNF-TrkB pathway contributes to cortical hemorrhage-induced depression, but not sex differences

Honglei Ren, Ranran Han, Xi Liu, Limin Wang, Raymond C Koehler and Jian Wang*

Abstract

Post-stroke depression, observed in 30-50% of stroke patients, negatively affects quality of life and mortality. The pathogenesis of post-stroke depression is complex, but heightened reactive oxygen species production and inflammation might be two key factors. We have reported that intracerebral hemorrhage (ICH) in cerebral cortex produces depression-like behavior in young male mice. Here, we found that mice lacking nuclear factor erythroid-derived 2-related factor 2 (Nrf2), a transcription factor that upregulates antioxidant proteins and trophic factors such as brain-derived neurotrophic factor (BDNF), had more severe depression-like behavior than wild-type mice at days 21 to 28 after cortical ICH (c-ICH). Moreover, the expression of Nrf2, heme oxygenase-1, BDNF, and TrkB were significantly decreased in wild-type mice after c-ICH. Interestingly, TP-500 (2 mg/kg), a potent Nrf2 inducer, decreased the inflammatory response and reactive oxygen species production on day 28 after c-ICH and improved depression-like behaviors. TrkB receptor antagonist ANA-12 abolished this anti-depression effect. Depression was more severe in female than in male wild-type mice after ICH, but TP-500 improved depression-like behavior in females. These results suggest that downregulation of Nrf2-BDNF-TrkB signaling contributes to development of post-stroke depression, and that Nrf2 inducer TP-500 might improve depression after c-ICH.

Keywords

Intracerebral hemorrhage, depression, Nrf2, BDNF, stroke

Received 21 December 2020; Revised 29 May 2021; Accepted 30 May 2021

Introduction

Depression is a prevalent neuropsychiatric complication of stroke that increases the risk of suboptimal recovery, recurrent vascular events, poor quality of life, and mortality.[1,2] In the last two decades, our understanding of its underlying pathophysiological mechanisms has progressed. We now know that in addition to psychosocial factors and genetic susceptibility,[3] the neuroinflammatory response plays a key role in development of post-stroke depression (PSD).[3–6] However, most studies of PSD have focused on ischemic stroke,[3,6–8] and considerably less is known about the mechanisms that contribute to PSD after hemorrhagic stroke in humans and animals.[9] Intracerebral hemorrhage (ICH) is the second most common subtype of stroke, with approximately 2 million cases worldwide per year.[10,11] Patients who experience ICH are known to develop PSD.[12–14] Selective serotonin reuptake inhibitors can prevent and treat PSD clinically, although they are effective in only one-third of patients.[15] Alarmingly, two large clinical studies showed that selective serotonin reuptake inhibitors are associated with increased microbleeds or ICH incidence.[16,17] Thus, identifying new

Department of Anesthesiology and Critical Care Medicine, The Johns Hopkins University, Baltimore, MD, USA

*Jian Wang is no longer affiliated with The Johns Hopkins University.

Corresponding author:
Raymond C Koehler, Department of Anesthesiology and Critical Care Medicine, The Johns Hopkins University School of Medicine, 600 North Wolfe Street, Blalock 1404, Baltimore, MD 21287, USA.
Email: rkoehler@jhmi.edu

drug targets for PSD that are specific for ICH patients is a pressing need.

Upon the onset of ICH, blood components enter the brain and activate innate and adaptive immune cascade responses. Substantial evidence has indicated that elevated reactive oxygen species (ROS) production and inflammation might be two key biochemical factors that underlie PSD.[3–6,9] The nuclear factor erythroid-derived 2-related factor 2 (Nrf2) regulates ROS and inflammatory responses by triggering the expression of protective enzymes and scavengers[18–20] that provide neuroprotection against ICH. Therefore, enhancing this endogenous system might provide a means to reduce PSD.

Brain-derived neurotrophic factor (BDNF), one of the Nrf2 target genes, was shown to produce antidepressant effects in behavioral models of depression.[21] Nrf2/BDNF signaling also has been implicated in the antidepressant-like effect produced by agmatine[22] and fluoxetine.[23] Because the neurobiologic mechanisms of PSD differ from those of other depression subtypes,[24] we do not yet know whether activation of Nrf2 mitigates PSD after ICH. Thus, the goal of this study was to determine whether dysregulation of the Nrf2/BDNF pathway contributes to the development of PSD. We evaluated this pathway by using Nrf2-null ($NRF2^{-/-}$) mice and by examining the effect of Nrf2 activator TP-500[25] on depression-like behavior in a mouse model of cortical ICH (c-ICH) that has been shown to produce depression-like behavior. We postulated that Nrf2 gene deletion would exacerbate PSD and that TP-500 would alleviate PSD. Furthermore, we tested whether blocking downstream BDNF signaling with a TrkB antagonist would block the protective effect of TP-500.

Material and methods

Animals

All experimental procedures were approved by the Institutional Animal Care and Use Committee at Johns Hopkins University School of Medicine and followed the Animal Research: Reporting In Vivo Experiments 2.0 (ARRIVE 2.0)[26] and the National Institutes of Health guidelines for the care and use of laboratory animals. We used 8- to 10-week-old C57BL/6 wild-type (WT) mice (male and female) and age-matched $Nrf2^{-/-}$ mice (on a C57BL/6 background). The $Nrf2^{-/-}$ mice were backcrossed regularly with pure C57BL/6 mice to avoid genetic drift. Unless otherwise specified below, the mice used in the experiments were all male. A total of 210 mice were used. Animals were randomized for treatment in a blinded manner by using the randomizer form at http://www.randomizer.org.[27] All efforts were made to minimize the number of animals used and to ensure minimal suffering. Outcomes were assessed by investigators blinded to group allocation. Mice were genotyped by PCR of genomic DNA that was isolated from tails.

Induction of ICH in mice

We used the collagenase-induced c-ICH model to produce depression-like behavior in mice.[28] For the ICH procedure, mice were anesthetized with isoflurane (3% initial, 1% to 1.5% maintenance) in O_2 and air (20%:80%). Under aseptic conditions, a midline scalp incision was made and a cranial burr hole (1 mm) was drilled into the right side of the skull (0.2 mm anterior and 1.5 mm lateral of bregma) A 30-gauge needle was then lowered into the cortex through the burr hole (1.2 mm ventral to the skull surface) for delivery of collagenase. The speed and volume of collagenase infusion were precisely controlled by a motorized microinjector (Stoelting, Wood Dale, IL). Mouse body temperature was maintained at $37.0 \pm 0.5\,^{\circ}C$ by the DC Temperature Controller (FHC Inc., Bowdoin, ME) throughout the experimental and early recovery periods.

Drug administration

To test the effect of Nrf2 activation, we used TP-500, a triterpenoid in the CDDO family (2-cyano-3-,12-dioxooleana-1,9 (11)-dien-28-oic acid) in which trifluoroethylamide is added to enhance blood-brain barrier permeability.[25] Mice were randomly assigned to receive TP-500 (2 mg/kg, Cayman Chemical, Ann Arbor, MI) or vehicle by gavage on day 7 post-ICH and then once daily until the experiment ended. This treatment strategy aimed to increase Nrf2 activation at a delayed time when the hematoma had mostly resolved.

The TrkB antagonist ANA-12 (Selleckchem, Houston, TX) was used to test the role of TrkB on the outcomes induced by TP-500. Mice were randomly assigned to receive isochoric ANA-12 or saline at a dose of 0.5 mg/kg by intraperitoneal injection from day 14 post-ICH until sacrifice. The start of the ANA-12 administration was delayed by 7 days from the start of TP-500 administration to allow the effects of Nrf-2 activation to be present when the TrkB receptors were blocked.

Behavioral assessment

Behavioral tests are widely used to assess sensorimotor function, cognitive function, and even affective changes in mice. In our study, a neurological deficit score was used to comprehensively evaluate the sensorimotor functions. Depression-like behavior was assessed with the forced swim test, the tail suspension test, and the

sucrose preference test. Cognitive deficits were evaluated with the novel object recognition test and the Y-maze test.

Neurological deficit score. Neurologic deficits of mice were evaluated by a 24-point scoring test system that assesses body symmetry, gait, climbing, circling behavior, front limb symmetry, and compulsory circling.[28] Each test was graded from 0 to 4, establishing a maximum deficit score of 24.

Forced swim test. Forced swim test is a rodent behavioral test used to evaluate "depression-like" behavior or behavioral despair, and it was carried out as previously reported.[28] Mice were acclimated to the behavior room for 1 h before being placed individually into a glass cylinder (20 cm high, 22 cm in diameter) containing 12 cm of water at 23-25°C for 6 min. Immobility in the last 4 min was assessed as a measure of depressive-like behavior. Mice were considered to be immobile if they were floating upright or making only movements necessary to keep their head above the water.

Tail suspension test. Tail suspension test is also a behavioral test measuring "depression-like" behavior or behavioral despair, and it was conducted as previously reported with minor modification.[28] Briefly, mice were acclimated to the behavior room for 1 h and then suspended by their tails at a height of 55 cm above the table. A camera recorded their movements for 6 min, and we used the last 4 min to determine the duration of immobility. Mice were considered immobile when they hung passively and completely motionless.

Sucrose preference test. Sucrose preference test is a reward-based test that is used as in indicator of anhedonia, which represents one of the core symptoms of depression. Each mouse was weighed and kept in a separate cage with two bottles of 1% sucrose solution for one day. Then, the bottles were changed to one containing 1% sucrose solution and one containing tap water for 4 days. The positions of the bottles were switched every day. The bottles were weighed at the beginning and end of the four days. The formula for calculating the sucrose preference was: sucrose consumption (g)/total liquid consumption × 100%. This test assumes that a lower sucrose preference corresponds to a more depressed state.

Novel object recognition test. The novel object recognition test is used to evaluate cognition, particularly recognition memory. The task procedures consist of three phases: habituation, training, and testing.[29] In brief, mice were habituated to an open field test apparatus for 10 min on the first day. Twenty-four hours later, in the training phase, mice were allowed to explore two identical novel objects (green cubes, 4 × 4 × 3 cm) for 5 min. After 1 h, they were exposed to one novel object (white ball, 5 cm in diameter) and one familiar object (green cube) for 5 min. All behavior was recorded on video. Exploration was defined as sniffing or touching the object with their noses or forepaws. A discrimination index was calculated as the total time spent with the new object/total time devoted to exploring objects × 100%.

Y-maze test. The Y-maze is widely used as a behavioral task to study spatial learning and memory. Testing occurs in a Y-shaped maze with three arms positioned at 120° angles to one another. The three identical arms were randomly designated as the start arm (always open), novel arm (blocked at the training, but open at the test), and other arm (always open). In the training phase, mice were allowed to explore only two arms (start arm and other arm) for 5 min. After 1 h, mice were placed back in the same start arm and had access to all three arms for 5 min. All behavior was recorded on video. Data were expressed as a discrimination index, which was calculated as the total time spent in the novel arm/total time spent in the novel arm and other arm × 100%.

Western blot analysis

Western blot analysis was used to assess the expression of Nrf2-BDNF-TrkB pathway proteins. On days 21 to 28 after c-ICH, mice were sacrificed after anesthesia with isoflurane, and the ipsilateral cortex of the brain was collected. Total proteins were extracted, electrophoresed, and transferred onto polyvinylidene fluoride membranes. After being blocked with 5% non-fat dry milk in TBST, membranes were probed with primary antibodies against Nrf2 (1:2000, Santa Cruz Biotechnology, Dallas, TX, sc-365949), heme oxygenase-1 (HO-1, 1:2000, Enzo Life Sciences, Farmingdale, NY, ADI-SPA-895-F), BDNF (1:2000, Invitrogen, Grand Island, NY, PA5-95183), TrkB (1:2000, Invitrogen, PA5-95244), phosphorylated p38 (1:1000, Cell Signaling Technology, 4511S), p-38 (1:1000, Cell Signaling Technology, 8690S), phosphorylated $ERK^{1/2}$ (1:2000, Cell Signaling Technology, 4370 T), $ERK^{1/2}$ (1:1000, Cell Signaling Technology, 4695 T), PI3K (1:1000, Cell Signaling Technology, 4257 T), phosphorylated AKT(1:1000, Cell Signaling Technology, 4060S), AKT (1:1000, Cell Signaling Technology, 4685S), and β-actin (1:5000, Santa Cruz Biotechnology, sc-47778) at 4 °C overnight followed by incubation with horseradish peroxidase–labeled anti-rabbit or anti-mouse secondary antibody (1:3000,

Santa Cruz Biotechnology) for 1 h. The intensity of protein bands was detected with an ImageQuant ECL Imager (GE Healthcare, Chicago, IL). Image J was used for image gray value analysis. All data were normalized to the corresponding loading control (β-actin) and expressed as fold change from the value of the sham mouse brain.

Real-time PCR

Total RNA was extracted from the ipsilateral cortex of brains with the miRNeasy Mini Kit (Qiagen, Hilden, Germany) according to the manufacturer's instructions. The concentration of RNA was quantified by ultraviolet spectrophotometry at 260/280 nm with a NanoDrop spectrophotometer (Thermo Fisher Scientific, Waltham, MA). cDNA was transcribed with a High-Capacity cDNA Reverse Transcription Kit (Thermo Fisher Scientific, Waltham, MA), and real-time PCR was carried out on an ABI 7500 Fast Real-Time PCR System (Applied Biosystems, Foster City, CA) with corresponding primers (Supplementary Table 1) and SYBR green PCR master mix (Roche Diagnostics, Basel, Switzerland). The expression levels of mRNA are presented as fold change (ΔΔCt) and normalized to that of the sham group.[30]

Immunofluorescence

Brain sections (25-μm thickness) were cut with a cryostat microtome (Leica, Wetzlar, Germany) and stained by standard immunohistochemistry procedures as previously described.[31] The primary antibodies for immunostaining were anti-BDNF (1:500, Bioss Antibodies, Woburn, MA, bs-4989R) and anti-TrkB (1:2000, Invitrogen, PA5-95244), anti-iNOS (1:100, BD Transduction Laboratories, 610,328). Images were captured with a Nikon Eclipse 90i fluorescence microscope, and immunofluorescent intensity and number of positive cells were analyzed with Image J. Images were captured from four optical fields at 20×10 magnification in each of three sections per animal. Cell densities were calculated per square millimeter. The average fluorescence intensity is expressed as fold change in the perihematomal area normalized to the sham group.

ROS detection

Dihydroethidium (DHE, Sigma-Aldrich, St. Louis, MO), which is oxidized to the red fluorescent molecule ethidium by superoxide, was used to detect *in situ* ROS production in cortex. In brief, mice were injected intraperitoneally with DHE (100 μL, 4 mg/mL) three times at 1 h intervals. Then mice were sacrificed and their brains collected and cut into sections (25-μm thickness). Finally, the brain sections were incubated with DAPI and observed under a microscope at 200x magnification.

A ROS fluorometric assay kit (Elabscience, Houston, TX) was used to detect total ROS production in the brain. According to the manufacturer's instructions, brains were mechanically rubbed with a nylon mesh to prepare single cell suspensions. A fluorescent probe was added to the suspension for detection on a plate reader at the emission wavelength of 525 nm.

Statistical analysis

Sample size was determined by power analysis using a significance level of $\alpha = 0.05$ and 80% power to detect significant differences. Data are presented as means ± SD. The Shapiro-Wilk test was applied for all the datasets to test for a normal distribution. Based on this test, Students *t*-test or Mann-Whitney tests were used for comparisons of two groups accordingly. For multigroup data that passed the normality test, one-way ANOVA followed by the Tukey *post hoc* test or two-way ANOVA followed by Bonferroni *post hoc* test was used. Values of $p < 0.05$ were considered statistically significant.

Results

Nrf2 knockout aggravates post-stroke depression, but not cognition impairment, after c-ICH

$Nrf2^{-/-}$ mice are known to develop larger lesion volumes and greater neurologic deficits than WT mice after striatal ICH.[32,33] Although depression-like behavior was not strictly correlated with cortical lesion volume after c-ICH,[28] we titrated the collagenase injected into the $Nrf2^{-/-}$ mice to match the lesion volume in WT mice and help ensure that our conclusions would not be confounded (Figure 1(a)). At day 1, we observed no significant difference in lesion volume between $Nrf2^{-/-}$ mice administered 0.15 μL of collagenase and WT mice administered 0.30 μL of collagenase. Neurological deficit scoring showed that sensorimotor deficits of $Nrf2^{-/-}$ and WT mice had mostly resolved by day 14 (Figure 1(b)). Therefore, the depression-like behaviors beyond 14 days appear not to be due to ongoing sensorimotor deficits in the c-ICH model.

We performed depression-like behavioral tests (forced swim test, tail suspension test, sucrose preference test) and cognition-like behavioral tests (novel object recognition test, Y-maze) between days 21 and 28, and found depression-like behavior and cognition deficits to be evident in both $Nrf2^{-/-}$ and WT mice after c-ICH when they were compared to the sham group (Figure 1(c) and (d)). However, $Nrf2^{-/-}$ mice

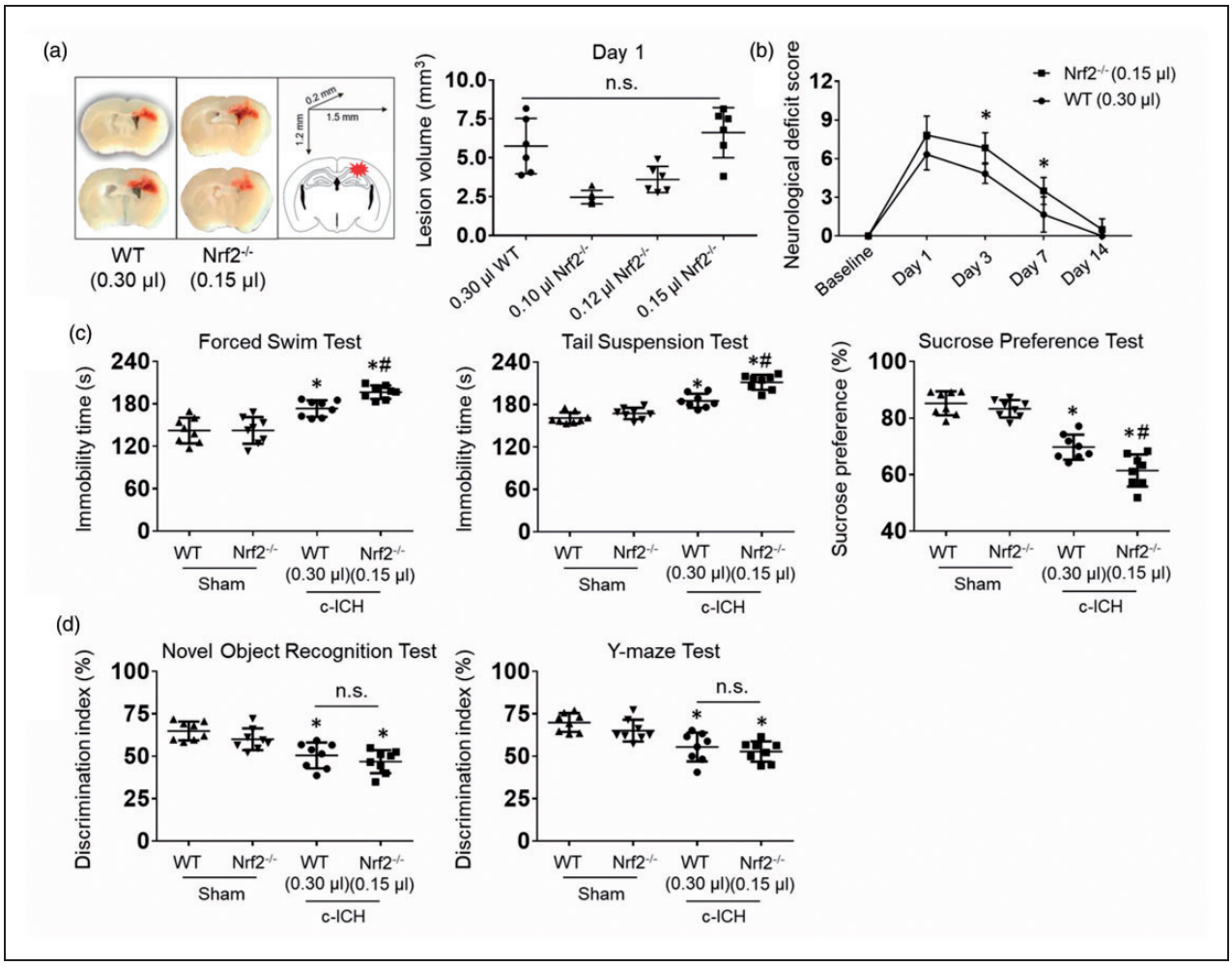

Figure 1. Nrf2 knockout exacerbates post-stroke depression, but not cognitive impairment, on days 21 to 28 after c-ICH. We titrated the collagenase dose injected into the $Nrf2^{-/-}$ mice until the lesion size matched that in WT male mice. (a) Representative images show matching lesion sizes on day 1 after c-ICH. (b) We measured neurologic deficits with a 24-point scoring system to evaluate sensorimotor function on days 1, 3, 7, and 14 after c-ICH. n = 6 mice/group, mean ± SD, $^{*}p < 0.05$ vs. WT. (c) Immobility time on the forced swim test and on the tail suspension test and the preference for sucrose over plain water were assessed during days 21–28 after sham surgery or c-ICH in male WT and $Nrf2^{-/-}$ mice. (d) Discrimination index in the novel object recognition test and Y-maze test. (C, D) n = 8 male mice per group, mean ± SD, $^{*}p < 0.05$ vs. sham of the same genotype; $^{\#}p < 0.05$ vs. c-ICH WT; n.s., not significant.

exhibited significantly longer immobility time in both the forced swim and tail suspension tests and had less sucrose preference than WT mice after c-ICH (Figure 1(c)). These results imply that lack of Nrf2 exacerbates the severity of PSD. In contrast, performance on the novel object recognition test and Y-maze test at this time period did not differ significantly between $Nrf2^{-/-}$ and WT mice (Figure 1(d)).

Nrf2-BDNF-TrkB pathway proteins decrease after c-ICH in WT mice

To investigate the possibility that the Nrf2-BDNF-TrkB pathway may be related to PSD, we harvested brain tissue at 28 days after c-ICH for western blotting or immunostaining of brain sections. Western blot measurement showed that expression levels of Nrf2, HO-1, BDNF, and TrkB were all markedly decreased 28 days after c-ICH (Figure 2(a) and (b)). In addition, quantification of immunostaining results showed that the expression levels of BDNF and TrkB were significantly downregulated on day 28 in the perilesion region (Figure 2(c) and (d)). Together, these data suggest a significant reduction in the Nrf2-BDNF-TrkB pathway after c-ICH.

Nrf2 inducer TP-500 ameliorates PSD after c-ICH

To examine whether Nrf2 activation can ameliorate PSD, we administered TP-500 (2 mg/kg) or vehicle

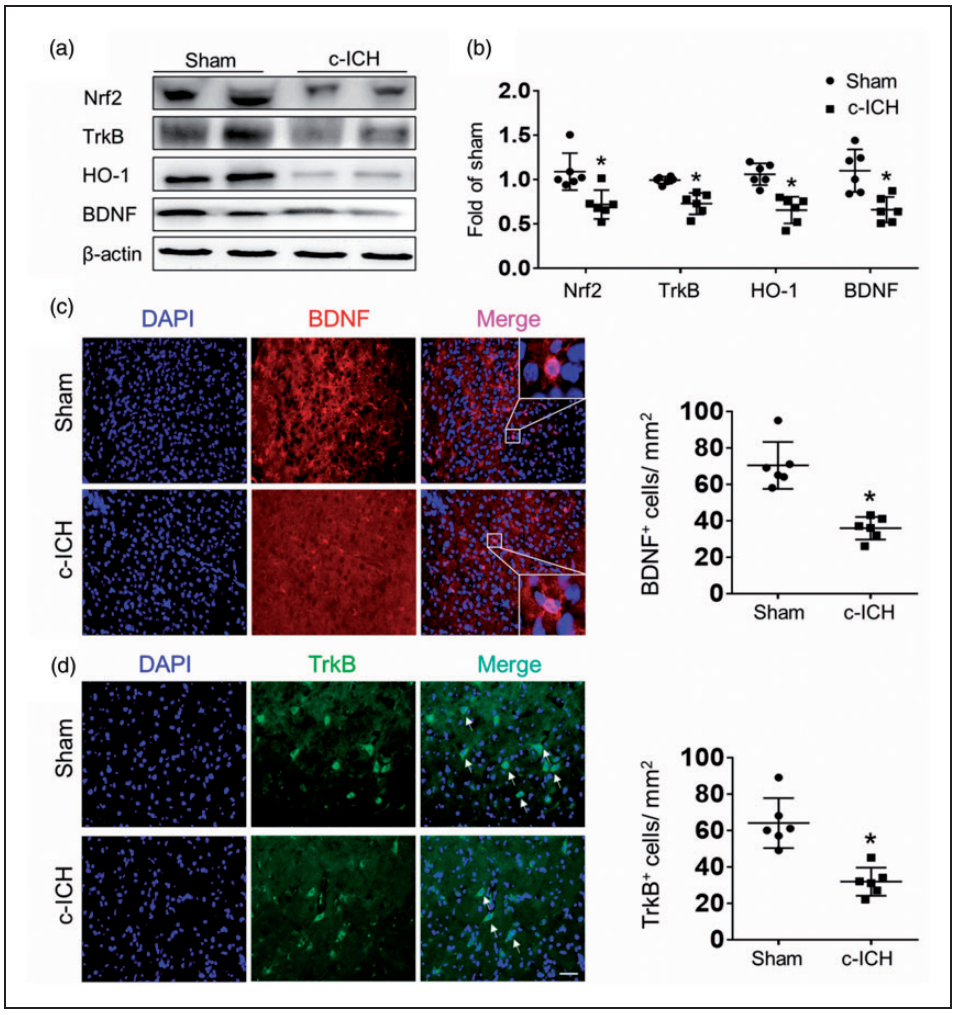

Figure 2. Expression levels of proteins in the Nrf2-BDNF-TrkB pathway decrease after c-ICH in WT mice. Representative immunoblot from WT mice (a) and quantification of optical density (b) showed a marked decrease in expression of Nrf2, HO-1, BDNF, and TrkB on day 28 after c-ICH. (c) Representative images and quantification of BDNF immunofluorescent intensity on day 28 after sham surgery or c-ICH. Scale bar = 50 μm. (d) Representative images and quantification of cells positive for TrkB immunoreactivity on day 28 after sham surgery or c-ICH. Scale bar = 50 μm. Values are mean ± SD; n = 6 male mice per group. *$p < 0.05$ vs. sham group.

starting on day 7 post-ICH and then once daily until the experiment ended. We then assessed depression-like behavior (Figure 3(a)). TP-500 treatment significantly attenuated the ICH-induced increase in immobility time on the forced swim and tail suspension tests, and largely restored performance on the sucrose preference test compared to that of the vehicle-treated group during days 21 to 28 after c-ICH (Figure 3(b)). No additional benefit on behavior outcome was observed at a higher dose of 10 mg/kg of TP-500 (Supplementary Fig. 1). Therefore, we used the 2 mg/kg dose in the remaining experiments. Western blot measurements showed that 2 mg/kg TP-500 treatment prevented the decrease in expression of Nrf2, TrkB, and BDNF that was seen in the vehicle-treated group (Figure 3(c)). To confirm whether TP-500 specifically activates Nrf2 pathways, we also performed depression-like behavioral tests during days 21 to 28 after c-ICH in $Nrf2^{-/-}$ mice receiving TP-500 or vehicle. The results showed that TP-500 administration in $Nrf2^{-/-}$ mice did not improve depression-like behaviors compared to the vehicle-treated group (Supplementary Fig. 2 A). In addition, western blot measurements showed that the increased expression of TrkB and BDNF with TP-500 treatment in WT mice was not evident in $Nrf2^{-/-}$ mice, indicating that the observed effects of TP-500 required the presence of Nrf2 (Supplementary Fig. 2B).

Nrf2 inducer TP-500 alleviates inflammatory responses and reduces ROS production after c-ICH

To further investigate the anti-PSD mechanism of TP-500, we evaluated the levels of brain inflammation after

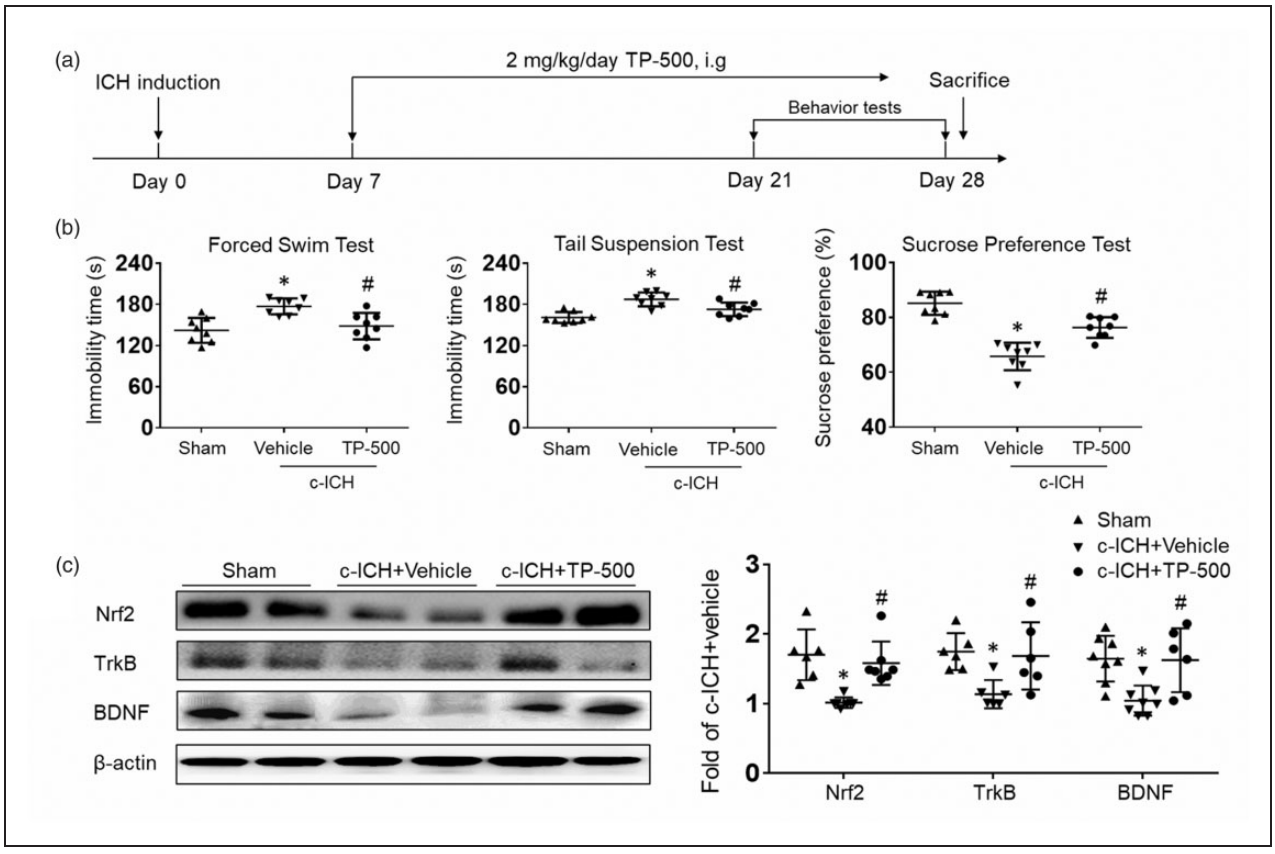

Figure 3. TP-500 treatment ameliorates post-stroke depression after c-ICH. Mice were treated with TP-500 (2 mg/kg) or vehicle on day 7 post-ICH and then once daily until the experiment ended. (a) Flow chart illustrates the timing of TP-500 administration and behavior testing. (b) TP-500 treatment significantly reduced immobility time on the forced swim test and on the tail suspension test and increased preference for sweetened drinking water after c-ICH. n = 8 male mice per group. (c) Western blot analysis showed that expression levels of Nrf2, TrkB, and BDNF were markedly higher in the TP-500 treatment group than in the vehicle group on day 28 after c-ICH. n = 6-8 male mice per group. Values are mean ± SD; $^{*}p < 0.05$ for vehicle vs. sham group; $^{\#}p < 0.05$ for TP-500 treatment vs. vehicle group.

c-ICH, as enhanced inflammation and ROS production might be key biochemical factors that underlie PSD.[4–7,10] We found that TP-500 treatment significantly decreased the mRNA expression of pro-inflammatory factors TNF-α, IL-6, and IL-1β, and increased the mRNA expression of anti-inflammatory factor IL-10 (Figure 4(a)). Additionally, DHE staining showed that ROS level in the vehicle group was significantly higher than that of the sham group on day 28 after c-ICH (Figure 4(b) and (c)). TP-500 treatment significantly reduced the level of ROS compared to that in the vehicle-treated group (Figure 4(b) and (c)). In addition, we found that TP-500 treatment also enhanced the expression of the antioxidant responsive element genes, NQO1, HMOX, and SOD1 (Supplemental Fig. 3). Taken together, these data indicate that TP-500 treatment alleviates the inflammatory responses and ROS that are implicated in PSD.

TrkB receptor antagonist ANA-12 abolishes the anti-depression effects of TP-500 after c-ICH

To determine whether TP-500 provides protection by targeting the TrkB receptor, we administered TrkB receptor antagonist ANA-12 to WT mice by intraperitoneal injection on day 14 post-ICH. As before, TP-500 was administered daily starting at day 7 (Figure 5 (a)). ANA-12 administration after TP-500 administration worsened depression-like behavior on the forced swim test, tail suspension test, and sucrose preference test, effectively blocking the benefit of TP-500 (Figure 5 (b)). Importantly, the expression of Nrf2 and BDNF was not reduced by ANA-12 treatment and remained elevated compared to that in a control c-ICH group (Figure 5(c)). These results indicate that the anti-PSD effects of TP-500 require TrkB receptors.

To further evaluate whether microglia/macrophage polarization may be linked to the downregulation of

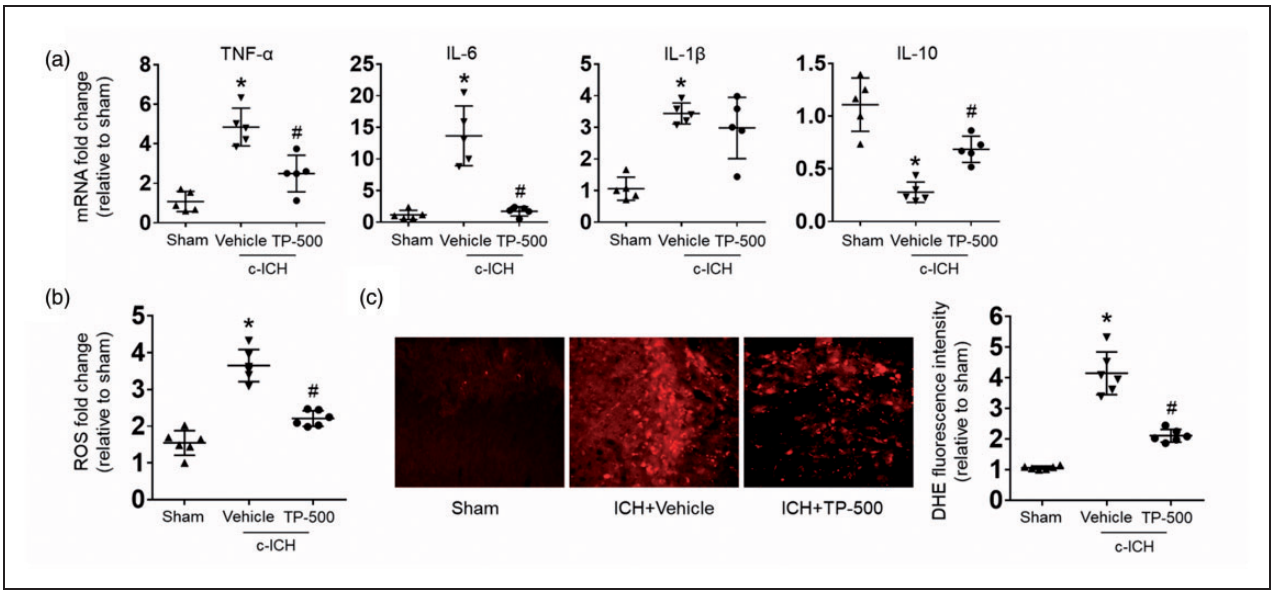

Figure 4. TP-500 treatment alleviates inflammatory responses and reduces ROS levels on day 28 after c-ICH. Mice were treated with TP-500 (2 mg/kg) or vehicle on day 7 post-ICH and then once daily until the experiment ended. (a) mRNA expression levels of inflammatory factors TNF-α, IL-6, IL-1β, and IL-10 on day 28 after c-ICH. TP-500 treatment reduced the expression of pro-inflammatory factors TNF-α, IL-6, and IL-1β, but increased the expression of anti-inflammatory factor IL-10. Dihydroethidium (DHE) fluorescence, a marker of ROS levels, was increased on day 28 after c-ICH compared to sham both when assayed ex vivo on cell suspensions (b) or in vivo after systemic injection (c). This increase was blunted by TP-500 treatment. n = 5–6 male mice per group. Values are mean ± SD; $^{*}p < 0.05$ for vehicle vs. sham group; $^{\#}p < 0.05$ for TP-500 treatment vs. vehicle group.

TrkB receptors after ICH, we measured the mRNA expression levels of microglia/macrophage polarization genes CD86 and CD206. TP-500 treatment significantly decreased the expression of pro-inflammatory gene CD86 and increased the expression of anti-inflammatory gene CD206. These changes were diminished by co-administration of ANA-12 (Figure 5(d)). Double-immunostaining results indicated that the colocalization of Iba-1^{+} and iNOS were significantly reduced after TP-500 treatment, whereas the decrease could be reversed by co-administration of ANA-12 (Figure 5(e)). These results further indicate that TP-500 treatment enhances antioxidant responses and reduces inflammation implicated in PSD, and the anti-PSD effects by TP-500 treatment after c-ICH requires TrkB receptors.

Next, we assessed the TrkB downstream MAPK and PI3K pathways by western blot. Increasing evidence supports a pivotal role of MAPK, in particular the extracellular signal-regulated kinase (ERK) subclass of MAPKs, in the pathogenesis, symptomatology, and treatment of depression.[34] Moreover, the regulation of PI3K/AKT/GSK3 signaling has also been implicated in the etiology of mood disorders and depression.[35] Our results showed that TP-500 treatment after c-ICH reduced the expression of phosphorylated p38 MAPK and augmented the expression of phosphorylated ERK$^{1/2}$ without altering the expression of total p38 or ERK (Figure 6(a) and (b)). The expression of PI3K and phosphorylated AKT also increased after TP-500 treatment (Figure 6(c) and (d)). Furthermore, ANA-12 co-administration reversed the TP-500–induced decrease in phosphorylated p38 MAPK and increase in phosphorylated ERK$^{1/2}$, PI3K and AKT. These results indicate that the TrkB-MAPK pathway and TrkB-PI3K pathway are both involved in therapeutic effect of TP-500.

Sex does not affect the expression level of Nrf2 or the therapeutic effect of TP-500

Increasing evidence suggests that females are at a greater risk for PSD and have more serious clinical symptoms than do males.[36] Therefore, we explored whether sex differences affect the expression level of Nrf2 after ICH, which might account for greater female susceptibility to PSD. First, we titrated the collagenase dose injected into the female mice to match the lesion volume in male mice and eliminate the influence of lesion volume on subsequent results. A higher dose of collagenase was required in female mice (0.35 μL, 0.053 U vs. 0.30 μL, 0.045 U) in order to match the lesion volume of the male mice (Figure 7(a)). On days 21 to 28 after c-ICH, we found more severe

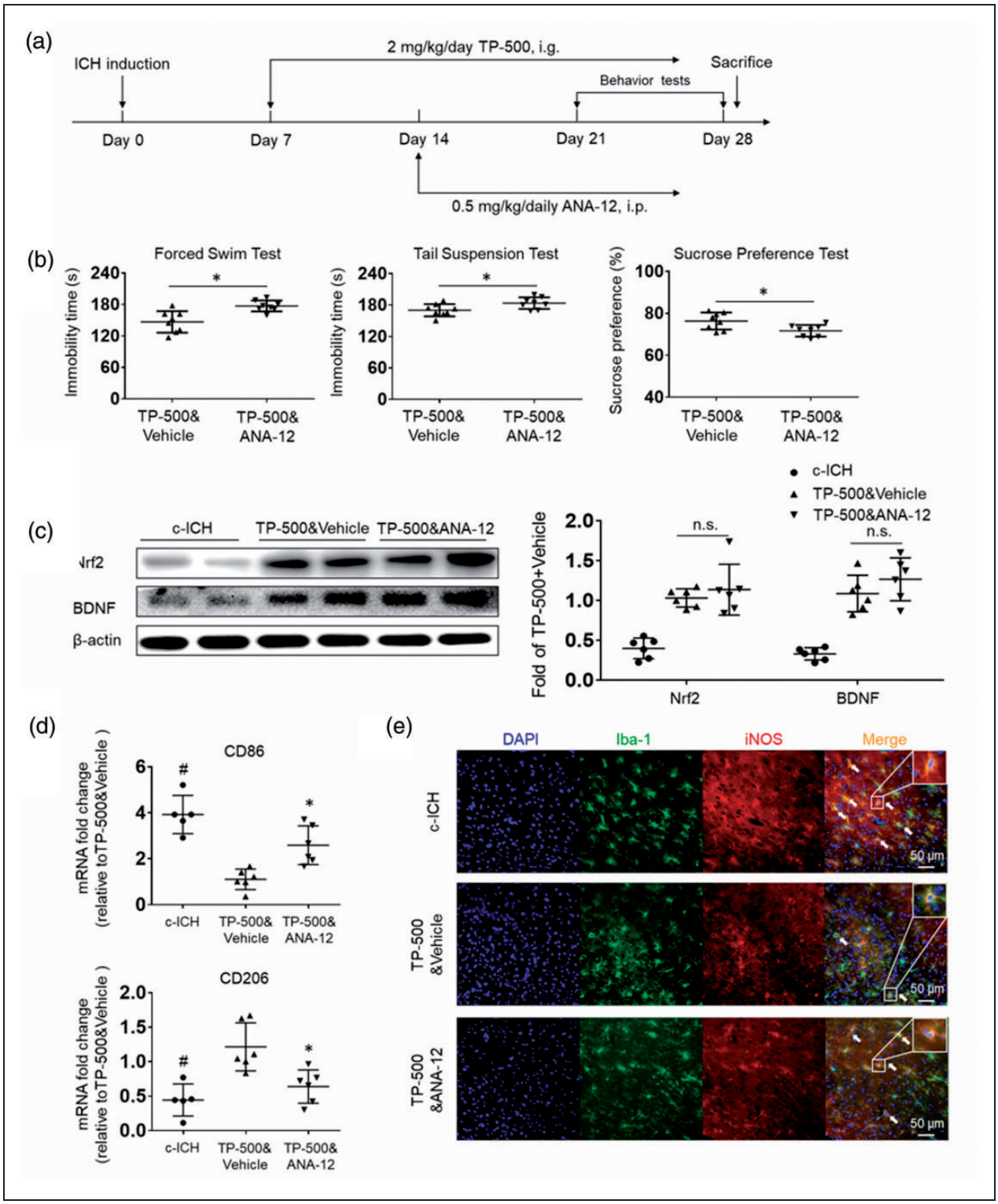

Figure 5. TrkB receptor antagonist ANA-12 blocks the anti-PSD effects of TP-500. Mice were treated with TP-500 (2 mg/kg) on day 7 post-ICH and then once daily until the experiment ended. ANA-12 (0.5 mg/kg) was administered on day 14 post-ICH and continued daily until the end of the experiment. (a) Flow chart illustrates the timing of the experimental protocol. i.p., intraperitoneal. (b) TP-500 treatment significantly reduced immobility time on the forced swim test and on the tail suspension test and increased preference for sweetened drinking water after c-ICH. These changes were abolished by concurrent administration of ANA-12. n = 8 male mice per group. Values are mean ± SD; *$p < 0.05$ for TP-500 & ANA-12 vs. TP-500 & vehicle. (c) Western blots show that the TP-500–induced increase in protein expression of Nrf2 and BDNF on day 28 after c-ICH was not attenuated by concurrent administration of ANA-12. n = 6 male mice per group. Values are mean ± SD; n.s., not significant. (d) The mRNA expression levels of CD86, a pro-inflammatory marker for microglia/macrophages, and CD206, an anti-inflammatory marker, in brain tissue on day 28 after c-ICH. n = 5–6 male mice per group. (e) Immunostaining showed the colocalization of Iba-1$^+$ microglia/macrophages and pro- inflammatory factor iNOS in different groups on day 28 after c-ICH. Scale bar = 50 μm. n = 5–6 male mice per group. Values are mean ± SD. *$P < 0.05$ TP-500&ANA-12 vs. TP-500&vehicle group. $^{\#}P < 0.05$ TP-500&vehicle vs. c-ICH group.

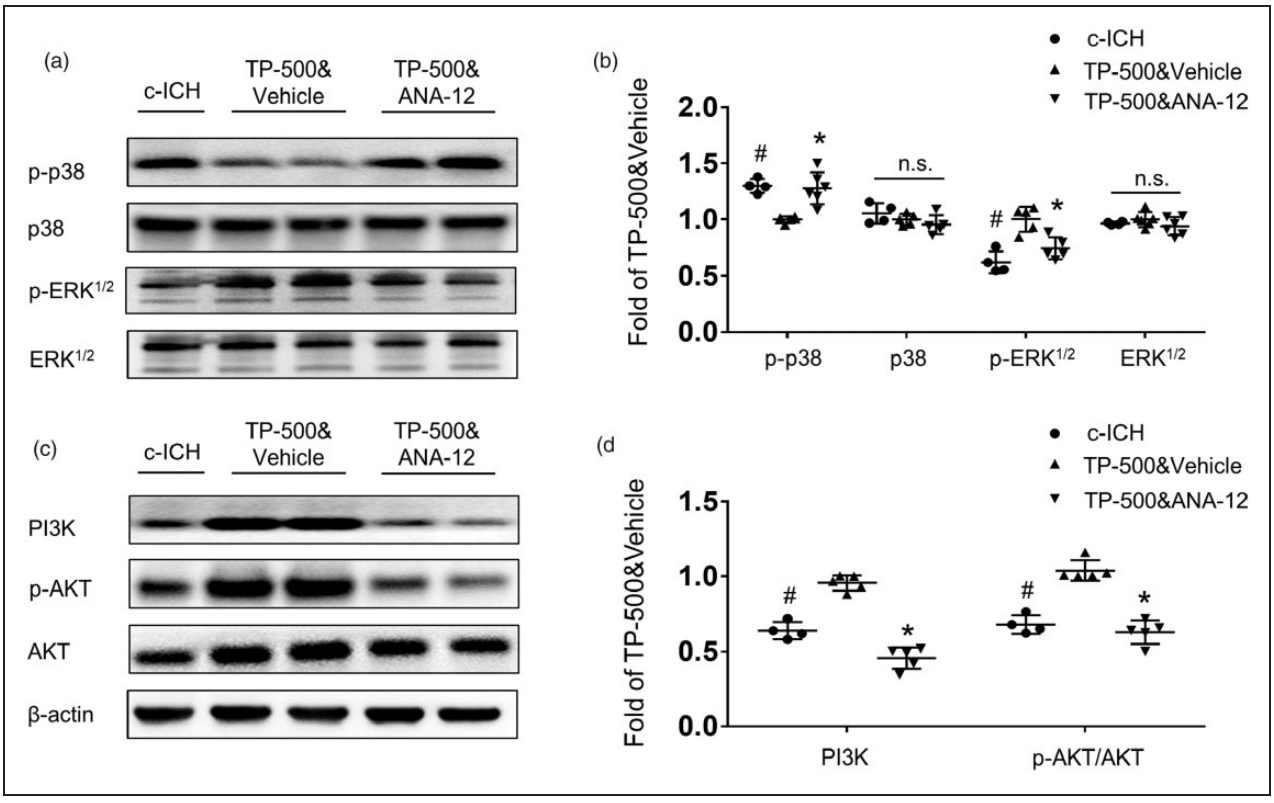

Figure 6. TP-500 treatment regulates TrkB downstream MAPK and PI3K pathways 28 days after c-ICH. (a and b) Western blots showed decreased expression of phosphorylated p-38 (p-p38) and increased expression of phosphorylated ERK$^{1/2}$ (p-ERK$^{1/2}$) after TP-500 treatment. These changes were abolished by co-administration of ANA-12. (c and d) Western blots showed increased expression of PI3K and phosphorylated AKT (p-AKT) after TP-500 treatment. Similarly, these changes were abolished by co-administration of ANA-12. n = 4-6 male mice per group. Values are mean ± SD. *$P < 0.05$ TP-500&vehicle vs. TP-500&ANA-12 group. #$P < 0.05$ TP-500&vehicle vs. c-ICH group.

depression-like behavior in female mice than in male mice (Figure 7(b)). No sex differences were seen in the expression levels of Nrf2, TrkB, or BDNF in the sham groups, and c-ICH decreased their expression equivalently in males and females (Figure 7(c)). Interestingly, TP-500 treatment significantly blunted the augmented depression-like behavior in the forced swim test, tail suspension test, and sucrose preference test compared to that of the vehicle-treated group in female mice on days 21 to 28 after c-ICH (Figure 7(d)).

Discussion

In this study, we observed that Nrf2 knockout significantly aggravates c-ICH–associated PSD without significantly affecting cognitive impairment. Expression of Nrf2, BDNF, and TrkB was markedly downregulated in the cortex after c-ICH. To determine the relationship between the Nrf2-BDNF-TrkB pathway and PSD, we administrated a potent, novel Nrf2 inducer, TP-500, to restore Nrf2 expression after c-ICH. Interestingly, TP-500 treatment significantly ameliorated depression-like behavior on the forced swim test, tail suspension test, and sucrose preference test on days 21 to 28 after c-ICH. TP-500 treatment was sufficient to reduce the mRNA levels of proinflammatory factors, such as TNF-α and IL-6, as well as ROS production. Furthermore, the benefit of TP-500 was diminished in mice treated with TrkB antagonist ANA-12. Taken together, these data underscore the importance of the Nrf2-BDNF-TrkB pathway in protecting against PSD under hemorrhagic conditions.

We used the collagenase-induced ICH model in our study because it can produce acute cerebrovascular injury with a reproducible hematoma in the desired brain region. When injected into the cortex of young male mice, collagenase has been shown to render depression-like behavior after resolution of the hematoma.[28] The pathogenesis of PSD is complex and multifactorial, and some neurobiologic mechanisms may differ from those in other depression subtypes.[24] Emerging evidence has shown that elevated ROS production and inflammation might be two key biochemical factors that underlie PSD. Lee et al.[37] hypothesized

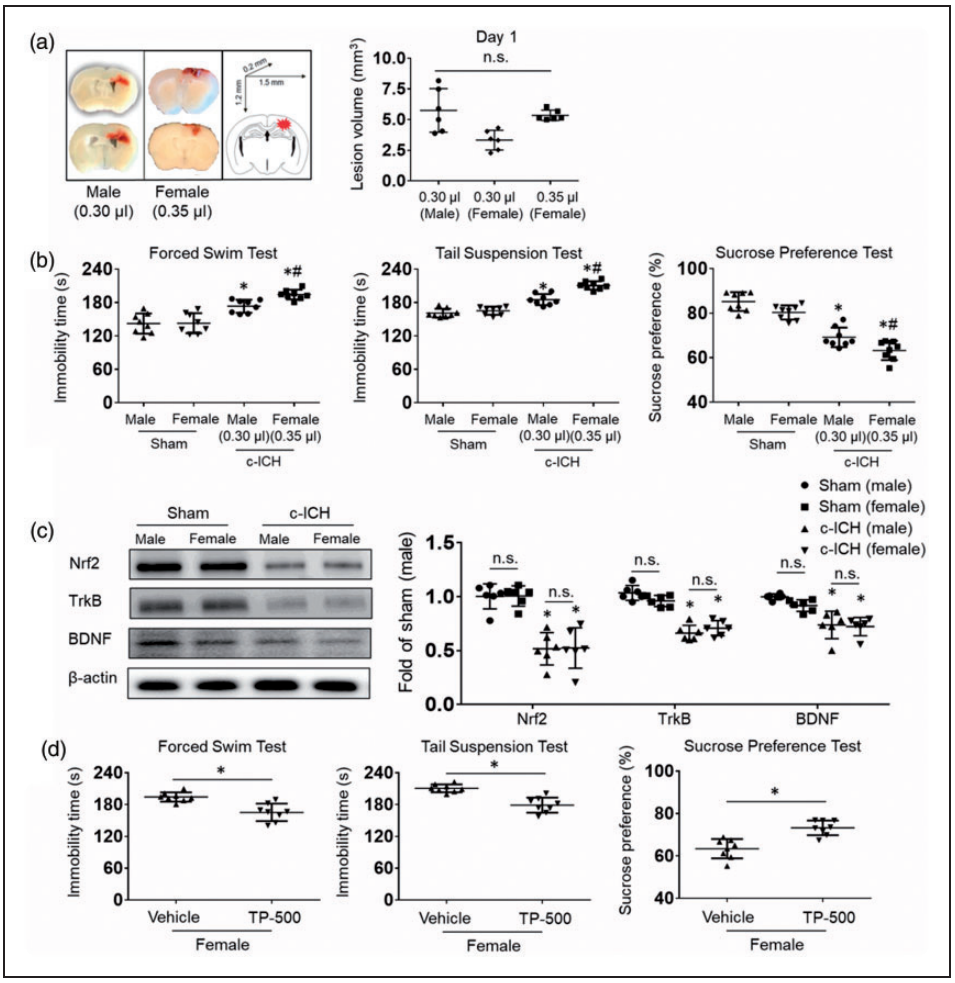

Figure 7. Sex does not affect the expression level of Nrf2 or the therapeutic effect of TP-500. (a) First, we titrated the collagenase injected into the female mice to match the lesion volume of male mice. Representative images show that a higher dose of collagenase was needed in female mice (0.35 µL, 0.053 U vs. 0.30 µL, 0.045 U) to match the lesion volume on day 1 after c-ICH. n = 6 mice/group. (b) Immobility time on the forced swim test and on the tail suspension test and preference for sweetened drinking water during days 21–28 after c-ICH was altered to a greater extent in female than in male WT mice. n = 8 mice per group. $^{*}p < 0.05$ vs. same sex sham; $^{\#}p < 0.05$ for female vs. male after c-ICH. (c) Western blots show that expression levels of Nrf2, TrkB, and BDNF were similar in male and female sham mice and decreased to a similar extent after c-ICH in the two sexes. n = 6 mice/group. (d) In female mice, TP-500 decreased immobility time on the forced swim test and on the tail suspension test and increased preference for sucrose in the drinking water during days 21–28 after c-ICH. n = 8 mice per group. Values are mean ± SD; $^{*}p < 0.05$ for TP-500 treatment vs. vehicle group; n.s., not significant.

that antioxidants could have clinical implications as future targets for depression treatments. Nrf2, a master regulator of oxidative stress and inflammatory responses, upregulates the expression of protective enzymes and scavengers[18–20] and also provides neuroprotection against ICH.[38,39] A recent clinical study showed that redox-sensitive transcription factors Nrf2 and NF-κB are upregulated in peripheral blood mononuclear cells of individuals with major depression.[40] In the past few years, several drugs have been found to provide antidepressant effects by influencing the Nrf2 signaling pathway in other depression models.[41,42] Additionally, the small molecule TP-500 significantly activates the Nrf2 pathway and produces neuroprotective effects in the Parkinson's disease model of MPTP neurotoxicity.[25] Our results demonstrate the ability of TP-500 to effectively reduce inflammatory responses and ROS levels in mice with ICH. Although Nrf2 activators have been evaluated for acute administration after ICH,[32,39] our data are unique in that administration of the Nrf2 activator was delayed by a week after ICH and the anti-inflammatory and antioxidant efficacy was demonstrated at 1 month.

The neurotrophic factor BDNF regulates neuronal survival and synaptic plasticity.[43] A decrease in BDNF is known to be associated with the pathophysiology of

depression, whereas increased BDNF is associated with the mechanisms underlying the actions of antidepressant drugs.[44] Indeed, the serum BDNF levels of patients with PSD are reported to be low before administration of antidepressant medications and to increase after administration.[45] Importantly, the effects of antidepressants can be abolished by BDNF depletion, and injection of exogenous BDNF can alleviate depression symptoms.[45] BDNF is a target gene of Nrf2,[46] and Nrf2/BDNF signaling is involved in the antidepressant-like effect produced by agmatine and fluoxetine.[47] In our study, we found that the decreased BDNF expression was congruent with that of Nrf2 in the brain at 28 days after c-ICH, and that the decrease could be reversed by TP-500. Our results demonstrate that TP-500 can effectively reduce pro-inflammatory cytokines (such as IL-6, TNF-α) and ROS levels. Accumulating evidence suggest that these pro-inflammatory cytokines and ROS may damage neuronal structure and function by suppression and reduction of BDNF.[48,49] Therefore, some anti-inflammatory drugs can exert antidepressant effects or enhance antidepressant effects.

TrkB is a receptor with high affinity for BDNF. Once BDNF binds to TrkB, ligand-mediated dimerization of the complex occurs at the cell surface, leading to activation of the downstream mitogen-activated protein kinase (MAPK), phosphatidylinositol-3-kinase (PI3K), and phospholipase Cγ (PLCγ) pathways. This activation of TrkB also aids in neurogenesis, gliogenesis, neurite outgrowth, and enhanced neuronal survival. Loss of BDNF-TrkB signaling leads to progressive degeneration of the nigrostriatal pathway.[50] Based on a postmortem study, Dwivedi et al.[51] reported that downstream components of BDNF/TrkB signaling, such as the MAPK and PI3K pathways, were also disrupted in subjects with depression. We found that BDNF/TrkB is essential for the beneficial effects of TP-500 treatment. TP-500 administration activates Nrf2, inhibits the production of pro-inflammatory cytokines and ROS, thereby promoting the antidepression effects of BDNF/TrkB. Moreover, activated BDNF/TrkB further mediates downstream MAPK and PI3K pathways, decreasing the expression of p-p38 MAPK and increasing the expression of p-ERK$^{1/2}$, PI3K and p-AKT. The production of inflammatory cytokines and oxidative stress can be regulated by the BDNF-TrkB-MEK-ERK pathway and the BDNF-TrkB-p38 MAPK pathway.[52] For example, upregulated of BDNF induced the protein expression of TrkB and suppressed p38 MAPK phosphorylation, thus reducing inflammation.[53] Once we blocked the TrkB receptor with ANA-12, the anti-PSD effects of TP-500 were abolished. When we view these data in light of its pharmacologic mechanism, we infer that TP-500 amelioration of c-ICH–induced depression was mediated mainly through preservation of the Nrf2-BDNF-TrkB pathway.

We also explored whether sex differences affect expression of Nrf2 after ICH. Increasing evidence suggests that females are at a greater risk for PSD and have more serious clinical symptoms than do males.[36] In our model, depression-like behavior was more severe in female mice than in male mice with similar initial lesion size. However, Nrf2 expression did not exhibit sex differences, either before or after ICH. Additionally, the beneficial effect of TP-500 on depression-like behavior was evident in both male and female mice despite the greater severity in female mice. Depression in females is often associated with changes in hormone levels, such as during postpartum and menopausal periods, and the prevalence of depression peaks at these times.[54,55] Thus, sex differences tend to diminish after menopause.[56] To further investigate the sex differences of PSD, we need to better understand how ICH affects estrogen and progesterone levels and the possible mechanisms. Nevertheless, TP-500 treatment could ameliorate PSD in young mice after c-ICH regardless of sex.

There are also some limitations in this study that should be addressed in future investigations. First, although we found the sex differences of PSD, the specific mechanisms remain to be explored. Second, we only used young mice in our study. Because the levels of BDNF and TrkB decrease with age,[57] the efficacy of an Nrf2 activator may decline with age. Third, our current study does not distinguish whether TP-500 can reverse depression symptoms once they are present or only prevents PSD from occurring. Delayed delivery of TP-500 needs to be evaluated in the future.

In conclusion, this study indicates that loss of Nrf2 exacerbates depression after ICH and that administration of the Nrf2 inducer TP-500 beginning one week after c-ICH attenuates brain inflammation and alleviates depression-like behavior in both male and female mice. The underlying mechanism appears to involve the Nrf2-BDNF-TrkB pathway. Therefore, delayed targeting of this pathway may serve as a promising antidepression strategy and warrants investigation in advanced preclinical ICH studies.

Funding

The author(s) disclosed receipt of the following financial support for the research, authorship, and/or publication of this article: This research was supported by grants from the National Institutes of Health NS101614, NS102583, and NS105894.

Declaration of conflicting interests

The author(s) declared no potential conflicts of interest with respect to the research, authorship, and/or publication of this article.

Authors' contributions

Honglei Ren was involved in the concept and design of the study, acquired and analyzed data, and drafted the manuscript; Ranran Han acquired and analyzed data; Xi Liu acquired and analyzed data; Limin Wang acquired and analyzed data; Raymond C Koehler revised the manuscript; Jian Wang conceived of the experimental design.

Supplementary material

Supplementary material for this paper can be found at the journal website: http://journals.sagepub.com/home/jcb

ORCID iD

Raymond C Koehler https://orcid.org/0000-0002-5890-9992

References

1. Hackett ML, Kohler S, O'Brien JT, et al. Neuropsychiatric outcomes of stroke. *Lancet Neurol* 2014; 13: 525–534.
2. Towfighi A, Ovbiagele B, El Husseini N, et al. Poststroke depression: a scientific statement for healthcare professionals from the American Heart Association/American Stroke Association. *Stroke* 2017; 48: e30–e43.
3. Robinson RG and Jorge RE. Post-stroke depression: a review. *Am J Psychiatry* 2016; 173: 221–231.
4. Spalletta G, Bossu P, Ciaramella A, et al. The etiology of poststroke depression: a review of the literature and a new hypothesis involving inflammatory cytokines. *Mol Psychiatry* 2006; 11: 984–991.
5. Wen H, Weymann KB, Wood L, et al. Inflammatory signaling in post-stroke fatigue and depression. *Eur Neurol* 2018; 80: 138–148.
6. Villa RF, Ferrari F and Moretti A. Post-stroke depression: mechanisms and pharmacological treatment. *Pharmacol Ther* 2018; 184: 131–144.
7. McCarthy MJ, Sucharew HJ, Alwell K, et al. Age, subjective stress, and depression after ischemic stroke. *J Behav Med* 2016; 39: 55–64.
8. Shen H, Tu X, Luan X, et al. Serum lipid profiles and post-stroke depression in acute ischemic stroke patients. *NDT* 2019; 15: 1573–1583.
9. Kronenberg G, Gertz K, Heinz A, et al. Of mice and men: modelling post-stroke depression experimentally. *Br J Pharmacol* 2014; 171: 4673–4689.
10. Keep RF, Hua Y and Xi G. Intracerebral haemorrhage: mechanisms of injury and therapeutic targets. *Lancet Neurol* 2012; 11: 720–731.
11. Zhu H, Wang Z, Yu J, et al. Role and mechanisms of cytokines in the secondary brain injury after intracerebral hemorrhage. *Prog Neurobiol* 2019; 178: 101610.
12. Cao H, Ju K, Zhong L, et al. Efficacy of hyperbaric oxygen treatment for depression in the convalescent stage following cerebral hemorrhage. *Exp Ther Med* 2013; 5: 1609–1612.
13. Christensen MC, Mayer SA, Ferran JM, et al. Depressed mood after intracerebral hemorrhage: the FAST trial. *Cerebrovasc Dis* 2009; 27: 353–360.
14. Koivunen RJ, Harno H, Tatlisumak T, et al. Depression, anxiety, and cognitive functioning after intracerebral hemorrhage. *Acta Neurol Scand* 2015; 132: 179–184.
15. Li C, Xu X, Wang Z, et al. Exercise ameliorates post-stroke depression by inhibiting PTEN elevation-mediated upregulation of TLR4/NF-κB/NLR3 signaling in mice. *Brain Res* 2020; 1736: 146777.
16. Akoudad S, Aarts N, Noordam R, et al. Antidepressant use is associated with an increased risk of developing microbleeds. *Stroke* 2016; 47: 251–254.
17. Renoux C, Vahey S, Dell'Aniello S, et al. Association of selective serotonin reuptake inhibitors with the risk for spontaneous intracranial hemorrhage. *JAMA Neurol* 2017; 74: 173–180.
18. Ma Q. Role of Nrf2 in oxidative stress and toxicity. *Annu Rev Pharmacol Toxicol* 2013; 53: 401–426.
19. Wang J, Jiang C, Zhang K, et al. Melatonin receptor activation provides cerebral protection after traumatic brain injury by mitigating oxidative stress and inflammation via the Nrf2 signaling pathway. *Free Radic Biol Med* 2019; 131: 345–355.
20. Liu L, Kelly MG, Wierzbicki EL, et al. Nrf2 plays an essential role in long-term brain damage and neuroprotection of Korean red ginseng in a permanent cerebral ischemia model. *Antioxidants (Basel* 2019; 8: 273.
21. Audet MC and Anisman H. Interplay between pro-inflammatory cytokines and growth factors in depressive illnesses. *Front Cell Neurosci* 2013; 7: 68.
22. Freitas AE, Egea J, Buendia I, et al. Agmatine, by improving neuroplasticity markers and inducing Nrf2, prevents corticosterone-induced depressive-like behavior in mice. *Mol Neurobiol* 2016; 53: 3030–3045.
23. Mendez-David I, Tritschler L, Ali ZE, et al. Nrf2-signaling and BDNF: a new target for the antidepressant-like activity of chronic fluoxetine treatment in a mouse model of anxiety/depression. *Neurosci Lett* 2015; 597: 121–126.
24. Feng C, Fang M and Liu XY. The neurobiological pathogenesis of poststroke depression. *ScientificWorldJournal* 2014; 2014: 521349.
25. Kaidery NA, Banerjee R, Yang L, et al. Targeting Nrf2-mediated gene transcription by extremely potent synthetic triterpenoids attenuate dopaminergic neurotoxicity in the mptp mouse model of parkinson's disease. *Antioxid Redox Signal* 2013; 18: 139–157.
26. Percie Du Sert N, Hurst V, Ahluwalia A, et al. The ARRIVE guidelines 2.0: updated guidelines for reporting animal research. *J Cereb Blood Flow Metab* 2020; 40: 1769–1777.
27. Cheng T, Wang W, Li Q, et al. Cerebroprotection of flavanol (-)-epicatechin after traumatic brain injury via Nrf2-dependent and -independent pathways. *Free Radic Biol Med* 2016; 92: 15–28.

28. Zhu W, Gao Y, Wan J, et al. Changes in motor function, cognition, and emotion-related behavior after right hemispheric intracerebral hemorrhage in various brain regions of mouse. *Brain Behav Immun* 2018; 69: 568–581.
29. Ampuero E, Stehberg J, Gonzalez D, et al. Repetitive fluoxetine treatment affects long-term memories but not learning. *Behav Brain Res* 2013; 247: 92–100.
30. Han X, Zhao X, Lan X, et al. 20-HETE synthesis inhibition promotes cerebral protection after intracerebral hemorrhage without inhibiting angiogenesis. *J Cereb Blood Flow Metab* 2019; 39: 1531–1543.
31. Li M, Ren H, Sheth KN, et al. A TSPO ligand attenuates brain injury after intracerebral hemorrhage. *FASEB J* 2017; 31: 3278–3287.
32. Zhao X, Sun G, Ting SM, et al. Cleaning up after ICH: the role of Nrf2 in modulating microglia function and hematoma clearance. *J Neurochem* 2015; 133: 144–152.
33. Wang J, Fields J, Zhao C, et al. Role of Nrf2 in protection against intracerebral hemorrhage injury in mice. *Free Radic Biol Med* 2007; 43: 408–414.
34. Wang JQ and Mao L. The ERK pathway: molecular mechanisms and treatment of depression. *Mol Neurobiol* 2019; 56: 6197–6205.
35. Beaulieu JM. A role for akt and glycogen synthase kinase-3 as integrators of dopamine and serotonin neurotransmission in mental health. *J Psychiatry Neurosci* 2012; 37: 7–16.
36. Schottke H and Giabbiconi CM. Post-stroke depression and post-stroke anxiety: prevalence and predictors. *Int Psychogeriatr* 2015; 27: 1805–1812.
37. Lee SY, Lee SJ, Han C, et al. Oxidative/nitrosative stress and antidepressants: targets for novel antidepressants. *Prog Neuropsychopharmacol Biol Psychiatry* 2013; 46: 224–235.
38. Lan X, Han X, Li Q, et al. (-)-epicatechin, a natural flavonoid compound, protects astrocytes against hemoglobin toxicity via Nrf2 and AP-1 signaling pathways. *Mol Neurobiol* 2017; 54: 7898–7907.
39. Zhao X, Sun G, Zhang J, et al. Dimethyl fumarate protects brain from damage produced by intracerebral hemorrhage by mechanism involving Nrf2. *Stroke* 2015; 46: 1923–1928.
40. Lukic I, Mitic M, Djordjevic J, et al. Lymphocyte levels of redox-sensitive transcription factors and antioxidative enzymes as indicators of pro-oxidative state in depressive patients. *Neuropsychobiology* 2014; 70: 1–9.
41. Zhu X, Liu H, Liu Y, et al. The antidepressant-like effects of hesperidin in streptozotocin-induced diabetic rats by activating Nrf2/ARE/glyoxalase 1 pathway. *Front Pharmacol* 2020; 11: 1325.
42. Yao W, Zhang JC, Ishima T, et al. Antidepressant effects of TBE-31 and MCE-1, the novel Nrf2 activators, in an inflammation model of depression. *Eur J Pharmacol* 2016; 793: 21–27.
43. Miranda M, Morici JF, Zanoni MB, et al. Brain-derived neurotrophic factor: a key molecule for memory in the healthy and the pathological brain. *Front Cell Neurosci* 2019; 13: 363.
44. Castren E. Neurotrophins and psychiatric disorders. *Handb Exp Pharmacol* 2014; 220: 461–479.
45. Zhang E and Liao P. Brain-derived neurotrophic factor and post-stroke depression. *J Neurosci Res* 2020; 98: 537–548.
46. Lee JM, Li J, Johnson DA, et al. Nrf2, a multi-organ protector? *FASEB J* 2005; 19: 1061–1066.
47. Kale M, Nimje N, Aglawe MM, et al. Agmatine modulates anxiety and depression-like behaviour in diabetic insulin-resistant rats. *Brain Res* 2020; 1747: 147045.
48. Xie ZM, Wang XM, Xu N, et al. Alterations in the inflammatory cytokines and brain-derived neurotrophic factor contribute to depression-like phenotype after spared nerve injury: improvement by ketamine. *Sci Rep* 2017; 7: 3124.
49. Calabrese F, Rossetti AC, Racagni G, et al. Brain-derived neurotrophic factor: a bridge between inflammation and neuroplasticity. *Front Cell Neurosci* 2014; 8: 430.
50. Baydyuk M, Nguyen MT and Xu B. Chronic deprivation of TrkB signaling leads to selective late-onset nigrostriatal dopaminergic degeneration. *Exp Neurol* 2011; 228: 118–125.
51. Dwivedi Y, Rizavi HS, Zhang H, et al. Modulation in activation and expression of phosphatase and tensin homolog on chromosome ten, Akt1, and 3-phosphoinositide-dependent kinase 1: further evidence demonstrating altered phosphoinositide 3-kinase signaling in postmortem brain of suicide subjects. *Biol Psychiatry* 2010; 67: 1017–1025.
52. Jin Y, Sun LH, Yang W, et al. The role of BDNF in the neuroimmune axis regulation of mood disorders. *Front Neurol* 2019; 10: 515.
53. Liang J, Deng G and Huang H. The activation of BDNF reduced inflammation in a spinal cord injury model by TrkB/p38 MAPK signaling. *Exp Ther Med* 2019; 17: 1688–1696.
54. Hahn-Holbrook J, Cornwell-Hinrichs T and Anaya I. Economic and health predictors of national postpartum depression prevalence: a systematic review, Meta-analysis, and Meta-regression of 291 studies from 56 countries. *Front Psychiatry* 2017; 8: 248.
55. Zeng LN, Yang Y, Feng Y, et al. The prevalence of depression in menopausal women in China: a meta-analysis of observational studies. *J Affect Disord* 2019; 256: 337–343.
56. Sonnenberg CM, Beekman AT, Deeg DJ, et al. Sex differences in late-life depression. *Acta Psychiatr Scand* 2000; 101: 286–292.
57. Wu SY, Pan BS, Tsai SF, et al. BDNF reverses aging-related microglial activation. *J Neuroinflammation* 2020; 17: 210.